Peptides Hot Paper

How to cite:
International Edition: doi.org/10.1002/anie.202108501
German Edition: doi.org/10.1002/ange.202108501

Histidine-Mediated Ion Specific Effects Enable Salt Tolerance of a Pore-Forming Marine Antimicrobial Peptide

Wujing Xian, Matthew R. Hennefarth, Michelle W. Lee, Tran Do, Ernest Y. Lee, Anastassia N. Alexandrova, and Gerard C. L. Wong**

Abstract: Antimicrobial peptides (AMPs) preferentially permeate prokaryotic membranes via electrostatic binding and membrane remodeling. Such action is drastically suppressed by high salt due to increased electrostatic screening, thus it is puzzling how marine AMPs can possibly work. We examine as a model system, piscidin-1, a histidine-rich marine AMP, and show that ion-histidine interactions play unanticipated roles in membrane remodeling at high salt: Histidines can simultaneously hydrogen-bond to a phosphate and coordinate with an alkali metal ion to neutralize phosphate charge, thereby facilitating multidentate bonds to lipid headgroups in order to generate saddle-splay curvature, a prerequisite to pore formation. A comparison among Na^+, K^+, and Cs^+ indicates that histidine-mediated salt tolerance is ion specific. We conclude that histidine plays a unique role in enabling protein/peptide-membrane interactions that occur in marine or other high-salt environment.

Introduction

Antimicrobial peptides (AMPs) contribute to innate immune defense against a broad spectrum of pathogens. AMPs can act via multiple antimicrobial functions, but one of the best known of these is their ability to preferentially permeate prokaryotic membranes rather than eukaryotic membranes.[1] With current challenges of antibiotic resistance and ultimately antibiotic tolerance in slow growing bacteria, the design principles of AMPs have emerged as an interesting conceptual starting point, since AMPs do not directly target growth processes as most antibiotics do (ex: cell wall synthesis, protein synthesis, DNA synthesis). One enduring mystery is how AMPs from marine organisms can possibly work in high salt environments, when typical AMP-membrane binding is drastically suppressed with increased electrostatic screening. Indeed, there have been efforts to engineer salt tolerant AMPs,[2] yet these peptides are structurally and functionally distinct from the large repertoire of AMPs discovered in marine organisms[3] which must work at levels of ionic strength found in oceans ($\approx$500 mM NaCl, in addition to other salts).

The occurrence of histidine is high in some marine AMPs (Table S1),[4] including piscidin 1 (Pis-1), but its function is not clear. We note that the function of histidine in peptides and proteins is often associated with pH sensitivity.[5] Moreover, it was recently suggested that histidines can enable antimicrobial activity by generating reactive oxygen species via Fenton chemistry.[6] There have also been studies on the role of histidines in the context of salt concentrations;[2b,5a] much more remains to be explored, however. Here, we examine Pis-1, a histidine-rich, α-helical AMP that originates in hybrid striped bass,[7] to see if and how the histidine residues maintain the function of Pis-1 in high salt concentrations. Differences in a given ion's ability to influence a broad range of protein behavior are often expressed in the Hofmeister series, and are recently rationalized in terms of specific interactions of hydrated salt ions with the sidechains and backbone of a protein.[8] To gain more insight into the role of Na^+ in marine pore-formers, it is in principle desirable to examine more generally the histidine-ion interaction via a Hofmeister series of alkali metal ions, i.e., Na^+, K^+ and Cs^+. A purely computational approach, however, involves a simultaneous compaction of difficulties: the multiscale nature of required ion-membrane simulations, the high salt concentrations, and the ion-specific effects.

In this work, we mitigate these difficulties by combining a simple implementation of density functional theory (DFT) with synchrotron small angle X-ray scattering (SAXS) to investigate membrane remodeling, mutational studies to assess the role of histidines, and antimicrobial assays to monitor the biological function. The combined results show that specific salt-histidine interactions play unanticipated but pivotal roles in marine AMP membrane remodeling activity: DFT calculations suggest that histidines can simultaneously H-bond to one phosphate and associate with a Na^+ ion to coordinate another phosphate, thereby facilitating multidentate histidine binding to two phospholipid

[*] W. Xian, M. W. Lee, T. Do, E. Y. Lee, Prof. G. C. L. Wong
Department of Bioengineering,
University of California, Los Angeles
Los Angeles, CA 90095 (USA)
E-mail: gclwong@seas.ucla.edu
M. R. Hennefarth, Prof. A. N. Alexandrova
Department of Chemistry and Biochemistry,
University of California, Los Angeles
Los Angeles, CA 90095 (USA)
E-mail: ana@chem.ucla.edu
Prof. A. N. Alexandrova, Prof. G. C. L. Wong
California Nano Systems Institute,
University of California, Los Angeles
Los Angeles, CA 90095 (USA)

headgroups. This structural arrangement is analogous to the multidentate H-bonds of arginine in cell penetrating peptides,[9] which promotes generation of negative Gaussian curvature (NGC) in membranes, the kind of curvature topologically required for membrane permeation processes like pore formation. We hypothesize that this effect, combined with salt-independent generation of positive mean curvature from hydrophobic insertion into the target membrane,[10] allows Pis-1 to be a potent AMP at high salt levels. Despite the simplicity of the computational framework, we find that it is consistent with a broad range of observed experimental results: When the histidines in Pis-1 are substituted with lysines (K) and arginines (R), the mutant becomes less effective in inhibiting bacterial growth at marine salt concentrations, despite gaining more cationic charges. Consistent with observed antimicrobial activity, the K/R-substituted mutant is less effective in generating NGC, the class of membrane curvature enabled by the Na^+ coordination from DFT, in model bacterial membranes at marine-level Na^+ concentrations compared to the wildtype Pis-1. Interestingly, we also find that placement of histidines near the hydrophilic-hydrophobic interface of the Pis-1 helix, where predicted ion coordination effects are in principle most impactful, is crucial for activity: When the histidine residues are moved to the center of the hydrophilic face, NGC generation is strongly suppressed. Experimental phase diagrams of Pis-1/membrane lipids/alkali halide salts (NaCl, KCl and CsCl) indicate a non-monotonic dependence of NGC generation on the cation size, which is inconsistent with a picture in which the primary contribution of salt is electrostatic screening. More generally, that histidine can mimic a multivalent cation even though it is essentially uncharged implies that it can interact with membranes and macromolecules in unexpected ways, especially at high salt concentrations.[11]

Results and Discussion

Designing Mutants to Assess the Role of Histidine and Its Locations in Pis-1-Mediated Membrane Remodeling

Pis-1 is an ideal AMP to illustrate the coordinating effect of histidine in the context of its salt tolerance. AMPs are often characterized by their cationic charge and hydrophobicity, although recent work has allowed more nuanced analysis of the amino acid composition.[14] Pis-1 (Figure 1a) is strongly hydrophobic (Table 1) but does not have typical levels of cationic charge in AMPs. We designed a Pis-1 analog, Pis-KR, by replacing all histidines with lysine (K) or arginine (R) (Figure 1b), both heavily used as the cationic component in non-marine AMPs. Comparing Pis-KR to Pis-1 allows us to assess histidine contribution to membrane remodeling as a function of different salt conditions. We designed another Pis-1 analog, Pis-mH, to evaluate the significance of the placement of the histidines at the hydrophilic-hydrophobic interface. In Pis-mH, histidines are moved from the hydrophilic-hydrophobic interface to the

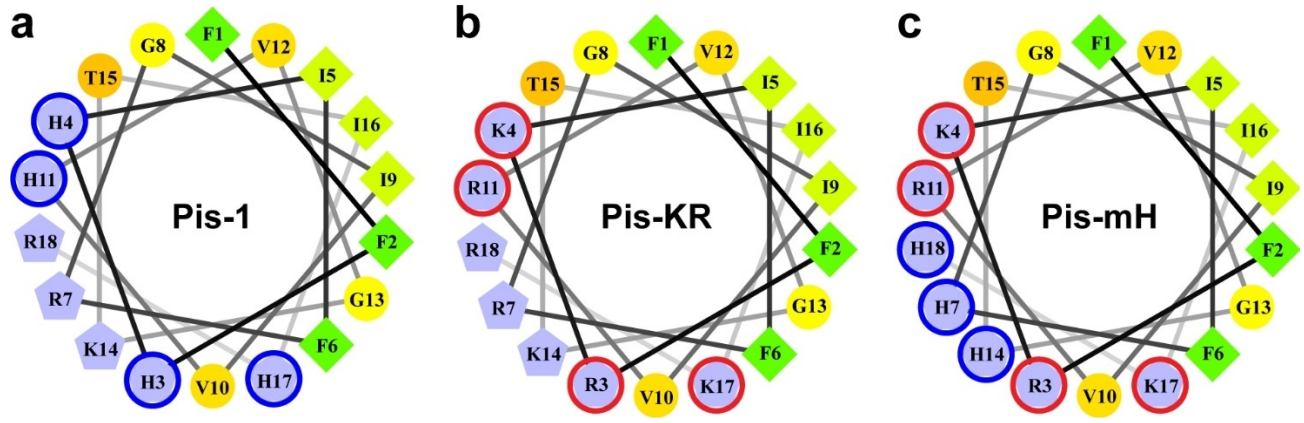

Figure 1. Designing Pis-1 analogs. a) Pis-1. Residues 1–18 are plotted on a helical wheel. The four histidines are at the hydrophilic-hydrophobic interface (blue circles). b) Pis-KR. Lysine and arginine (red circles) are placed at the hydrophilic-hydrophobic interface. c) Pis-mH. Lysine and arginine (red circles) are placed at the hydrophilic-hydrophobic interface, and histidines (blue circles) are placed in the middle of the hydrophilic face.

Table 1: Properties of Pis-1, Pis-KR and Pis-mH.

Peptide	Sequence	pI[a]	Charge[a]	⟨H⟩[b]	⟨μH⟩[b]
Pis-1	FFHHIFRGIVHVGKTIHRLVTG-NH_2	11.84	4.0	0.695	0.622
Pis-KR	FFRKIFRGIVRVGKTIKRLVTG-NH_2	12.32	7.9	0.469	0.747
Pis-mH	FFRKIFHGIVRVGHTIKHLVTG-NH_2	12.85	5.0	0.639	0.584

[a] The isoelectric point pI and the charge at pH 7.5 are calculated using the Protein Isoelectric Point Calculator.[12] [b] The mean hydrophobicity ⟨H⟩ and the mean helical hydrophobic (amphipathic) moment ⟨μH⟩ are calculated using HeliQuest with residues 1–20.[13]

middle of the hydrophilic face (thus "-mH") (Figure 1c). The helical hydrophobic moment of Pis-1, Pis-KR and Pis-mH are comparable, whereas at pH 7.5 the amount of positive charges for Pis-KR (+7.9) is ≈2x as much as Pis-1 (+4), and that for Pis-mH (+5) is one more than Pis-1 (Table 1). We confirmed that the mutant peptides Pis-KR and Pis-mH have similar helix-forming propensities as the wild-type peptide Pis-1: Using circular dichroism, we observed very similar random coil-to-helix transformation for all three peptides with added detergent, and that the helical conformations for all three peptides in detergent were also very similar (Figure S1).

Antimicrobial Activities of Pis-1, Pis-KR and Pis-mH against Gram-Positive Bacteria at High Salinity

Minimum inhibitory concentration (MIC) assays were carried out on Gram-positive bacteria *Staphylococcus epidermidis* and *Staphylococcus aureus.* High concentrations of NaCl affects *S. epidermidis* and *S. aureus* cultured in normal nutrient broth (LB or TSB). *S. epidermidis* precipitates at 500 mM NaCl, whereas the growth of *S. aureus* decreases as NaCl concentration increases. Therefore, the bacteria were first allowed to adapt to growing in high salt levels by repeated growth in increasing NaCl concentrations.[15] Once adapted, the bacteria grew to similar density overnight as measured by OD_{600} in NaCl concentrations of 100–500 mM. In parallel, we added 5 mM $MgCl_2$ to reflect the presence of Mg^{2+} in the marine environment, and similar growth as a function of different NaCl concentrations was observed with or without Mg^{2+}.

In the absence of Mg^{2+} (Figure 2a), the activity of Pis-1 is sustained up to 400 mM NaCl, and only starts to decrease at 500 mM NaCl; the activity of Pis-KR is similar to Pis-1 at 100–200 mM NaCl but starts to decrease at 300 mM NaCl; the activity of Pis-mH is weaker than both Pis-1 and Pis-KR at all NaCl concentrations except the lowest at 100 mM.

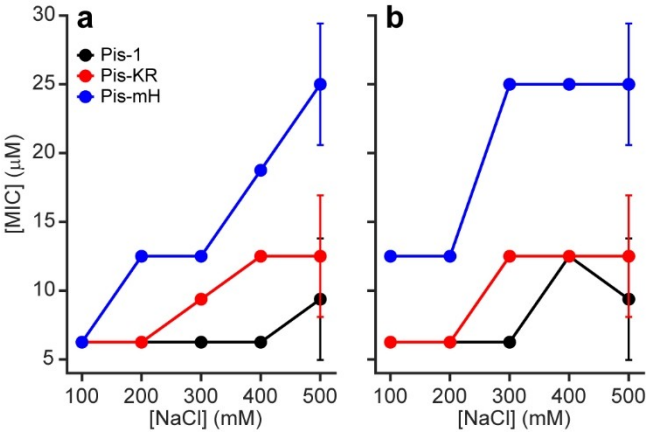

Figure 2. MIC measurements for Pis-1, Pis-KR and Pis-mH against *S. epidermidis.* a) MIC in 0 mM Mg^{2+}. *S. epidermidis* was adapted to grow in LB with 500 mM NaCl. b) MIC in 5 mM Mg^{2+}. *S. epidermidis* was adapted to grow in LB with 500 mM NaCl and 5 mM $MgCl_2$.

Similar trends are observed in the presence of 5 mM Mg^{2+} (Figure 2b): Pis-1 sustains its activity up to 300 mM NaCl before decreasing, Pis-KR sustains its activity up to 200 mM NaCl before decreasing, and the activity of Pis-mH is significantly weaker than both Pis-1 and Pis-KR at all NaCl concentrations tested. This pattern of antimicrobial activities towards *S. epidermidis* is also observed for *S. aureus* (Figure S2). The MIC results for Gram-positive bacteria show two surprising trends: 1) Pis-1 sustains its antibacterial activity better than Pis-KR at high NaCl concentrations, despite the fact that Pis-KR has almost twice as many positive charges as Pis-1, affirming the importance of histidine for salt tolerance in Pis-1; and 2) Pis-mH has overall diminished antibacterial activity compared to Pis-1 and Pis-KR, despite the fact that Pis-mH has one more positive charge than Pis-1.

We examine these observed MIC trends via fundamental arguments on ion-peptide interactions. The propensity for multidentate bonding by arginine has been correlated to the generation of NGC in phospholipid membranes, either via H-bond interactions to multiple phosphate groups[9b] or through multiple contact points with phosphate and carbonyl groups.[16] NGC is geometrically necessary for membrane permeation mechanisms associated with antimicrobial activity, such as pore formation and budding, and has been observed for typical AMPs at ≈100 mM NaCl, a criterion consistent with recent machine learning and bioinformatics studies.[14]

Histidine Can Mediate "Multidentate" Interactions with Phosphates by Coordinating with a Na^+ at High Salinity

To investigate how histidines in Pis-1 interact with phospholipid headgroups in NaCl, we next construct a minimal, quantum mechanical model using DFT calculations. We probe the coordination of the alkali cation to histidine, and then of $HisX^+$ (X^+ represents alkali metal ions) and protonated lysine to Cl^- ions in solution and the phosphate groups present in the membrane. Firstly, binding two anions (whether Cl^-, or $H_2PO_4^-$) rather than just one was found to be preferred for both $HisX^+$ and lysine (Table S2 and Table S3). We computed the $\Delta\Delta G$ of the association with the anions (with positive indicating preference to binding two chlorines) and versus the dielectric constant (since it is not known precisely for the studied peptide-membrane complexes) in Figure 3a. Note that inaccuracies in the computed free energies are expected due to the implicit treatment of the solvent, particularly impacting Cl^- that would have to undergo a desolvation with a large entropic penalty upon association. For this reason, Lys is taken as a reference for all trends in Figure 3a. For all $HisX^+$ complexes, there is a strong preference to bind two phosphates instead of two chlorines, as compared to lysine. The cation partially neutralizes the negatively charged phosphate groups, allowing the neutral histidine to hydrogen bond with one of the phosphates. Additionally, the cation binds to histidine's π-system resulting in a multidentate structure that successfully binds two phosphates (Figure 3b

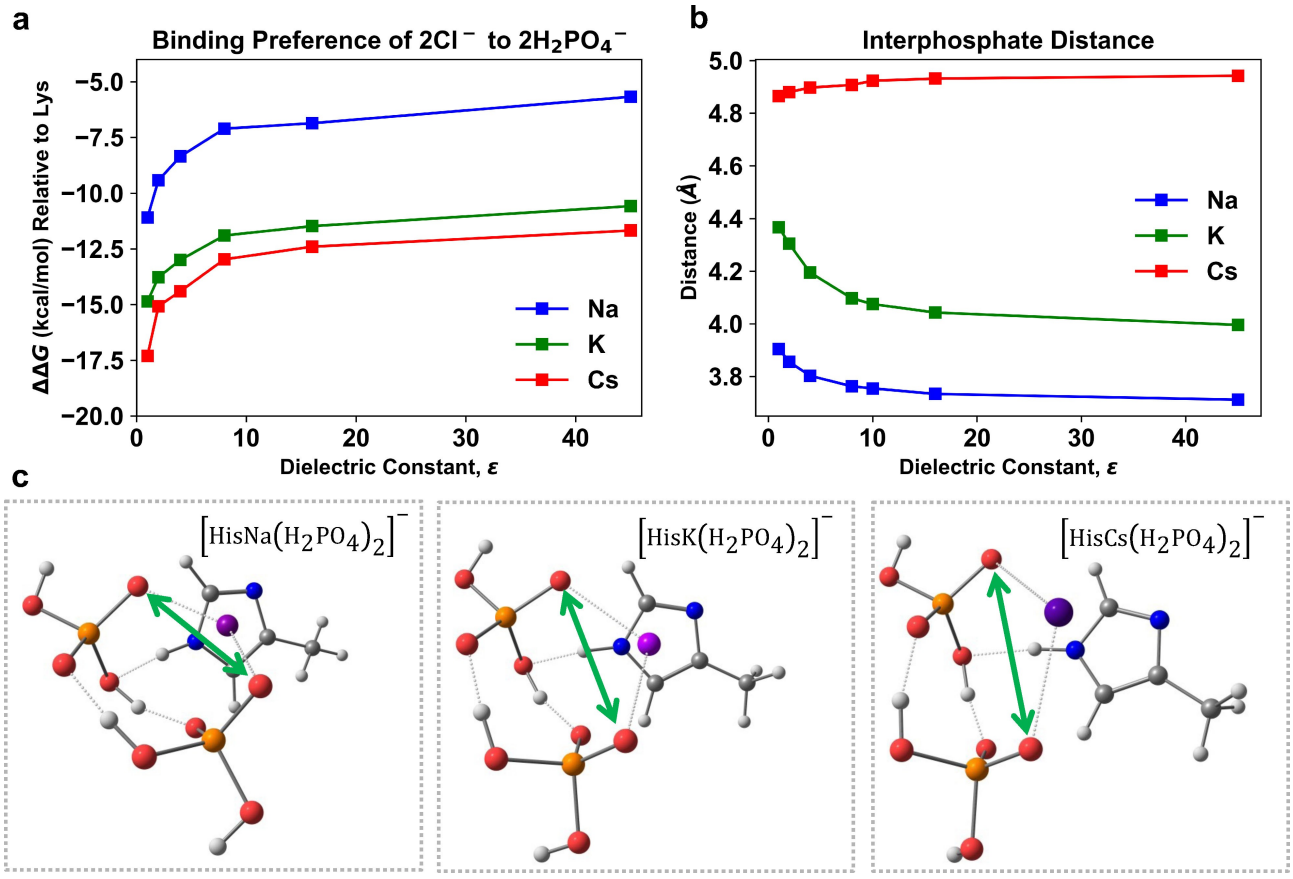

Figure 3. Relative binding of two chlorines to two phosphates for lysine and histidine bound with various cations. a) $\Delta\Delta G$ for the reaction of $HisX^+$ with either two Cl^- or two $H_2PO_4^-$ relative to lysine. Positive $\Delta\Delta G$ indicates preference for lysine to bind phosphates over $HisX^+$. b) Interphosphate distance, i.e. distance between two negatively charged oxygens bound to cation, as indicated by green arrows in (c), as a function of the dielectric. Notice that distance between the two negatively charged oxygens increases down the Hofmeister series at all dielectrics. c) Optimized structures of histidine bound to $2(H_2PO_4)^{2-}$ with Na^+, K^+, and Cs^+ in the gas phase. The cation is bound to histidine's π-system forming a multidentate ligand.

and Figure 3c, see also Figure S3 and Figure S4)). In general, $Cs^+ > K^+ > Na^+$ bound with histidine is the trend for binding affinity of free phosphates, which follows the Hofmeister series. This trend most likely arises from the difference in the increased ionic radii of the cation present. For a small cation, like Na^+, the distance between the two negatively charged phosphates is decreased, whereas for larger cations like K^+ and Cs^+, there is greater distance between the charged phosphates (Figure 3b). An increase in the distance between these negatively charged groups will decrease the electrostatic repulsion and enhance the binding of the histidine. Our model is minimalistic, and additional constraints could exist when the phosphate groups are attached to the lipid membrane; specifically, the proximity of two phosphate groups upon association with $HisX^+$ or Lys might be restricted. This could reduce interphosphate repulsion and further facilitate the association when the cations are small, i.e. Na^+. Additionally, we hypothesize that there is an optimal distance between the two phosphate groups which will allow for generation of NGC, and sufficient binding to the histidine residue.

There are, however, two predictions that can be made based on these calculations: 1) It is possible for histidine to employ a distinct mechanism at high salt concentrations for coordinating with multiple phosphates on lipid headgroups. This multidentate coordination has been previously correlated to membrane curvature generation.[9] 2) Both histidine-ion-phosphate binding and resultant membrane curvature generation will depend on the specific monovalent ion, which is an unexpected result.

Quantifying Membrane Remodeling by Pis-1 Mutants

To compare with the predictions from our simple DFT computational framework, we investigated the NGC-inducing ability of Pis-1, Pis-KR and Pis-mH in order to assess directly if changes in biological activity track with membrane remodeling at high salt. To that end, we developed a model membrane system consisting of small unilamellar vesicles (SUVs)[14b,17] with a composition of PG/PE/CL 20/60/20 that is found to be suitable for high salt concentrations (up to 600 mM) for SAXS experiments (Supporting Information). Alkali metal ions Na^+, K^+ and Cs^+ were used for comparison. Mg^{2+} at 2.5 mM was also included to access its effect. We note that although Mg^{2+} ions are known to bridge

lipid headgroups,[18] their concentrations here are not sufficiently high to influence membrane curvature significantly. In order to focus on Pis-1-mediated membrane remodeling relevant to antimicrobial activity, we examined structural transitions at a peptide-to-lipid (P/L) molar ratio of 1/25, just below the MIC.[19] Examples of SAXS spectra and peak indexing are illustrated in Figure 4, and the results are summarized in Table 2.

Interestingly, in NaCl concentrations ranging from 100–600 mM, only Pis-1 generated cubic phases in PG/PE/CL 20/60/20 SUVs. For examples, at 250, 400 and 600 mM NaCl, SAXS spectra for SUVs that were exposed to Pis-1 exhibited correlation peaks with Q-ratios of $\sqrt{2} : \sqrt{3} : \sqrt{4} : \sqrt{6} : \sqrt{8} : \sqrt{9}$ which are indexed to a Pn3m cubic phase (Figure 4). Bicontinuous lipidic cubic phases, such as the Pn3m "double diamond" cubic lattice here, are also induced by classical AMPs rich in lysines and arginines with model bacterial membranes.[17b,c] A bicontinuous cubic phase consists of two nonintersecting aqueous pore networks separated by a lipid bilayer with NGC at every point on its surface. In other words, Pis-1 remodels membranes with a bacterial-like composition by inducing NGC, which is the type of curvature that is geometrically required for membrane permeabilization events. These results suggest that Pis-1 has the capacity to kill bacteria via direct, physical membrane disruption even at high salt concentrations.

Strikingly, under the same conditions, Pis-KR does not generate cubic phases or any other high curvature phases. At 100 mM NaCl, the SAXS spectrum (data not shown) exhibits a set of correlation peaks with integral Q-ratios consistent with a periodicity of 4.39 nm, which indicate the formation of a lamellar (L_α) phase without significant curvature. This result indicates that Pis-KR binds electrostatically to anionic membranes and intercalates between bilayers to maximize contact with oppositely charged lipid headgroups. However, even in this extreme case of Pis-KR-membrane interaction, Pis-KR does not generate curvature, resulting instead in a flat lamellar phase. As NaCl concentrations increase (250–600 mM), electrostatic binding between Pis-KR and membranes is progressively weakened. Consistent with this picture, the diffraction signal evolves from that of a lamellar phase of bilayers with intercalated Pis-KR to that of a form factor for isolated bilayer membranes at higher salt levels (Figure 4a and Table 2). This striking difference between Pis-1 and Pis-KR is a strong indication that Pis-1 employs a different NGC-generating mechanism than Pis-KR, one that is based on His-Na^+-phosphate coordination, which is active even at high NaCl concentrations. In replacing histidines with K/R in the mutants, one consideration is the "snorkel" effect of the long sidechains of K/R. It has been noted that since the sidechain of histidine is shorter than that of either lysine or arginine, it will not snorkel.[7d] This implies that His-rich peptides may not insert as deeply into the membrane and will require more hydrophobicity for the same membrane curvature generation. Coincidentally, bulky hydrophobic residues such as tryptophan, phenylalanine, and tyrosine are frequently found in His-rich marine AMPs. In our framework, the more superficial arrangement of histidines allows better access to Na^+ ions, and thereby enhances curvature generation via a mechanism optimized for high salt. From a more general perspective, it will be interesting to explore conditions in which the Pis-KR mutant can generate NGC better than the less cationic Pis-1, given Pis-KR's higher cationic charge which is often a criterion for AMP-like membrane remodeling activity.

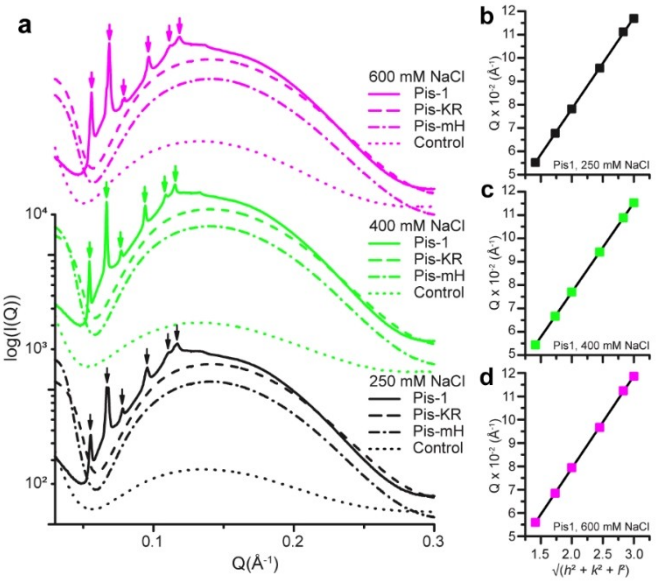

Figure 4. SAXS of Pis-1, Pis-KR and Pis-mH with PG/PE/CL 20/60/20 SUVs at various NaCl concentrations. a) SAXS spectra for Pis-1, Pis-KR, Pis-mH and control. The measured peak positions for Pis-1 at 250 mM NaCl (b), 400 mM NaCl (c) and 600 mM NaCl (d) are linearly fitted to the Pn3m cubic space group.

Table 2: Summary of SAXS results at P/L ratio of 1/25.

[Salt] (mM)	Pis-1			Pis-KR			Pis-mH			Control		
	Na^+	K^+	Cs^+	Na^+	K^+	Cs^+	Na^+	K^+	Cs^+	Na^+	K^+	Cs^+
100	C[a]	C	C	Lα	C	C + Lα	Lα	C	C + Lα	FF	FF	FF
250	C	C	C	FF	C	C	FF	C	FF	FF	FF	FF
400	C	C	C	FF	C	C	FF	C	FF	FF	FF	FF
500	C	C	C	FF	C	C	FF	C	FF	FF	FF	FF
600	C	C	C	FF	C	C	FF	C	FF	FF	FF	FF

[a] Abbreviation: C = Cubic phase, L_α = Lamellar phase, FF = Form factor.

Next we compare the NGC-inducing ability of WT Pis-1 with that of Pis-mH, on which the histidines have been moved from the amphiphilic interface immediate adjacent to the hydrophobic face to the middle of the hydrophilic face. Pis-mH has slightly higher charge at pH 7.5 (+5) than Pis-1 (+4), but less than Pis-KR (+7.9) (Table 1). At 100 mM NaCl, Pis-mH only induces a lamellar phase with a periodicity of 4.36 nm without inducing membrane curvature, and it is not able to generate a cubic phase at higher NaCl concentrations (Figure 4a and Table 2), in contrast to Pis-1. In this part of the phase diagram, the data is consistent with form factors characteristic of SUVs (Figure 4a). Under these conditions (in NaCl, with a P/L ratio of 1/25), Pis-mH behaves similarly to Pis-KR, rather than Pis-1. It is clear that placement of histidines near the hydrophilic-hydrophobic interface of the Pis-1 helix is crucial for its high-salt antimicrobial activity. This observation suggests that histidine-mediated reorganization of headgroup volume is most impactful near the hydrophilic–hydrophobic interface, which is qualitatively consistent with previous studies of lipid phase behavior using lipids synthesized with hydrophobic substituents with altered volumes adjacent to the carbonyl group of the fatty acyl chain.[20] Moreover, it was found in computer simulations that Pis-1 can generate positive mean curvature, presumably from hydrophobic insertion into the target membrane.[10] Indeed, positive curvature is one of the necessary ingredients of NGC, which has positive curvature along one principal direction and negative curvature in the other; this is consistent with the structural tendencies we observe. By engineering Pis-mH, we hypothesized that in order to generate NGC, the placement of histidines on Pis-1 must be close to the hydrophobic face, so that the membrane curvature generated from histidine coordination with phosphates can be combined with that from insertion of hydrophobic residues into the lipid bilayer. The observation that Pis-mH, the histidines of which are no longer in close proximity of the hydrophobic face, fails to generate NGC is consistent with our hypothesis.

The Role of Specific Ions on Pis-1-Mediated Membrane Remodeling via Histidine Sidechain Interactions

DFT calculations and SAXS measurements highlight a novel role for ions in marine AMPs: Rather than simply contributing to electrostatic screening, the coordination of a monovalent ion with histidine is crucial for its bidentate interactions with phospholipids that contribute to NGC generation. Differences in a specific ion's ability to influence a broad range of protein behavior are often expressed in the Hofmeister series, and are rationalized in terms of specific interactions of hydrated salt ions with the sidechains and backbone of a protein. Indeed, DFT calculations above suggest that K^+ has an even greater propensity than Na^+ to form the histidine-ion-phosphate coordination necessary for NGC generation. Here, we test whether such ion specific effects exist in Pis-1 to mediate NGC generation, by investigating its activity in NaCl, KCl, and CsCl salt solutions of different concentrations.

At a modest molar ratio of P/L = 1/25, Pis-1 can generate NGC in NaCl, KCl, and CsCl up to 600 mM salt concentration, as indicated by the induced restructuring of PG/PE/CL 20/60/20 SUVs into cubic phases (Table 2). In a cubic phase, the average amount of Gaussian curvature in the unit cell, $\langle k \rangle$, can be calculated via $\langle k \rangle = 2\pi\chi/a^2A_0$, where the Euler characteristic, χ, and the surface area per unit cell, A_0, are constants specific to each cubic phase, and a is the lattice parameter. For *Pn3m*, $\chi = -2$ and $A_0 = 1.919$.[21] For Na^+, Pis-1 generates a *Pn3m* cubic phase with a value of $\langle k \rangle$ that saturates near $-2.6\times10^{-2}\,nm^{-2}$ ($a_{Pn3m} \approx 15.9$ nm) at 600 mM NaCl. For K^+, more NGC is generated at high salt, and the corresponding saturation value of $\langle k \rangle$ is $-3.4\times10^{-2}\,nm^{-2}$ ($a_{Im3m} \approx 17.8$ nm) at 600 mM KCl. This is consistent with the DFT results, in which histidine-ion-phosphate coordination is found to be more favorable for K^+ than for Na^+.

To test the idea further, we examine Pis-mH, which has lost much of its NGC inducing capacity due to the suboptimal placement of histidines. For Na^+, we do not observe induction of high curvature phases: An L_α phase with no induced membrane curvature at 100 mM, and only the form factor of SUVs at all higher salt concentrations (250–600 mM). In contrast, we do observe weak NGC generation for K^+, which shows that K^+ is more amenable for NGC generation than Na^+. This is again in agreement with expectations from DFT calculations. Moreover, the value of $\langle k \rangle$ for Pis-mH is $-2.5\times10^{-2}\,nm^{-2}$ ($a_{Pn3m} \approx 16.2$ nm) at 600 mM KCl, which is lower in magnitude than the corresponding values for Pis-1 WT ($-3.4\times10^{-2}\,nm^{-2}$), as expected. Interestingly, for Cs^+ ions, we begin to see non-monotonic behavior with ion size. DFT calculations suggest even more energetically favorable histidine-ion-phosphate coordination, but due to the larger ion size and polarizability, and the likely distortions of the membrane, we do not expect the model to be predictive in this regime. Experimentally, we find that a weak cubic phase is generated, but only at 100 mM salt ($\langle k \rangle \approx -1.6\times10^{-2}\,nm^{-2}$, $a_{Pn3m} \approx 20.4$ nm). At all higher salt concentrations, only a form factor consistent with SUVs is observed, which indicates a decreased tendency for Cs^+ to induce NGC compared to K^+.

Membrane remodeling processes are known to be complex and multifactorial. For example, it has been shown that histidine, in particular H17 near the C-terminus of Pis-1, is important for piscidin membrane insertion.[7d] In agreement with that study, we find that membrane permeation activity is suppressed in Pis-mH, a mutant in which H17 is relocated (Figure 2). However, that such effects are observed in Na^+ but not in K^+ (Table 2) argues for the importance of both histidine-ion-phosphate coordination and insertion-promoting placement of histidine for the high salt activity of Pis-1.

Membrane remodeling processes that lead to pore formation has been studied for decades, and no clear consensus has emerged. In the prototypical case of cell penetrating peptides (CPP) for example, comparisons between experiments have been complicated by the use of different lipid compositions and by whether CPP has been conjugated to cargo, which can change the phsical chemistry

of the process.[9a] Generally, it appears that unconjugated CPPs and CPPs conjugated with cargo can access distinct but overlapping repertoires of entry mechanisms.[9a,22] In this study, we focus on what different remodeling processes have in common: A pore of any structure that connects the two sides of a membrane, whether a thermally-assisted transient pre-pore or a persistent pore, must exhibit NGC, which is the saddle-shaped curvature that makes the interior of pores possible. Since NGC is a combination of positive and negative curvatures in perpendicular principal directions, it is generally possible to correlate effects in specific systems to the capacity to generate positive or negative curvature.[23] Our goal here is to show how histidine-rich peptides can generate this type of curvature in high salt: We show experimentally and theoretically that ion coordination by histidine can result in membrane curvature. For example, the steric size of the coordinated ion and the ion coordination chemistry will both play roles in determining the final membrane curvature. We illustrated these ion-specific effects via a phase diagram of experimental results (Table 2 and Figure 4), which delineate in detail the necessary conditions for generating NGC in our specific system of His-rich peptides and biological membranes under high monovalent ion concentrations.

In a more general compass, the results presented here have potential application to marine pore-forming mechanisms outside of innate immune processes. For example, pore formation is central to biological processes such as sperm-egg fertilization. Given the pivotal role played by histidine in pore formation in high salt, it is interesting to examine the question of whether proteins associated with pore-forming machinery in the reproductive system of a given organism have amino acid content that is optimized for poration in salt water or fresh water, potentially providing a perspective to understand why it is necessary for anadromous fish to migrate to fresh water to spawn while catadromous fish migrate to salt water to spawn.

Conclusion

In summary, we elucidated a mechanism for membrane curvature generation in high-salt marine environments via Hofmeister-like effects. Specifically, we dissect a marine AMP, Pis-1, by analyzing the role of histidine-ion-phosphate coordination in NGC generation in lipid membranes by mutant AMPs and provide a general mechanism for the functioning of histidine-rich marine membrane remodeling peptides at high salt levels. These results establish a conceptual framework in which ions make AMP membrane remodeling activity possible, rather than just attenuate activity via electrostatic screening. Moreover, ion-specific effects (example: the foundational biological partitioning of Na^+ vs. K^+) can have unanticipated outcomes through histidine-ion-phosphate coordination in the extreme ionic environments of sea water.

Acknowledgements

We acknowledge helpful discussions with Myriam Cotten. This work used the Extreme Science and Engineering Discovery Environment (XSEDE) Bridges system at the Pittsburgh Supercomputing Center (PSC). A.N.A. acknowledges the support of the NSF CHE-1903808 grant and the NIH 1R01GM134047 grant. W.X., M.W.L., and G.C.L.W. are supported by NIH R01AI143730, NIH R01GM067180, and NSF DMR1808459. E.Y.L. acknowledges support from the Systems and Integrative Biology Training Program (NIH T32GM008185), the Medical Scientist Training Program (NIH T32GM008042), and the Dermatology Scientist Training Program (NIH T32AR071307) at UCLA. Use of the Stanford Synchrotron Radiation Lightsource (SSRL), SLAC National Accelerator Laboratory, is supported by the U.S. Department of Energy, Office of Science, Office of Basic Energy Sciences under Contract No. DE-AC02-76SF00515. The SSRL Structural Molecular Biology Program is supported by the DOE Office of Biological and Environmental Research, and by the National Institutes of Health, National Institute of General Medical Sciences (including P41GM103393).

Conflict of Interest

The authors declare no conflict of interest.

Keywords: Antimicrobial Peptide · Histidine · Hofmeister Series · Ion-Specific · Membrane

[1] L. Yang, V. D. Gordon, D. R. Trinkle, N. W. Schmidt, M. A. Davis, C. DeVries, A. Som, J. E. Cronan, Jr., G. N. Tew, G. C. Wong, *Proc. Natl. Acad. Sci. USA* **2008**, *105*, 20595–20600.

[2] a) H. Y. Yu, C. H. Tu, B. S. Yip, H. L. Chen, H. T. Cheng, K. C. Huang, H. J. Lo, J. W. Cheng, *Antimicrob. Agents Chemother.* **2011**, *55*, 4918–4921; b) J. Mai, X. L. Tian, J. W. Gallant, N. Merkley, Z. Biswas, R. Syvitski, S. E. Douglas, J. Ling, Y. H. Li, *Antimicrob. Agents Chemother.* **2011**, *55*, 5205–5213.

[3] G. Wang, X. Li, Z. Wang, *Nucleic Acids Res.* **2009**, *37*, D933–D937.

[4] a) A. J. Mason, P. Bertani, G. Moulay, A. Marquette, B. Perrone, A. F. Drake, A. Kichler, B. Bechinger, *Biochemistry* **2007**, *46*, 15175–15187; b) I. H. Lee, Y. Cho, R. I. Lehrer, *Infect. Immun.* **1997**, *65*, 2898–2903.

[5] a) S. Y. Kim, F. Zhang, W. Gong, K. Chen, K. Xia, F. Liu, R. Gross, J. M. Wang, R. J. Linhardt, M. L. Cotten, *J. Biol. Chem.* **2018**, *293*, 15381–15396; b) L. Kacprzyk, V. Rydengard, M. Morgelin, M. Davoudi, M. Pasupuleti, M. Malmsten, A. Schmidtchen, *Biochim. Biophys. Acta Biomembr.* **2007**, *1768*, 2667–2680; c) A. J. Mason, C. Gasnier, A. Kichler, G. Prevost, D. Aunis, M. H. Metz-Boutigue, B. Bechinger, *Antimicrob. Agents Chemother.* **2006**, *50*, 3305–3311.

[6] M. D. J. Libardo, A. A. Bahar, B. Ma, R. Fu, L. E. McCormick, J. Zhao, S. A. McCallum, R. Nussinov, D. Ren, A. M. Angeles-Boza, M. L. Cotten, *FEBS J.* **2017**, *284*, 3662–3683.

[7] a) X. Lauth, H. Shike, J. C. Burns, M. E. Westerman, V. E. Ostland, J. M. Carlberg, J. C. Van Olst, V. Nizet, S. W. Taylor, C. Shimizu, P. Bulet, *J. Biol. Chem.* **2002**, *277*, 5030–5039;

b) E. Y. Chekmenev, B. S. Vollmar, K. T. Forseth, M. N. Manion, S. M. Jones, T. J. Wagner, R. M. Endicott, B. P. Kyriss, L. M. Homem, M. Pate, J. He, J. Raines, P. L. Gor′kov, W. W. Brey, D. J. Mitchell, A. J. Auman, M. J. Ellard-Ivey, J. Blazyk, M. Cotten, *Biochim. Biophys. Acta Biomembr.* **2006**, *1758*, 1359–1372; c) B. S. Perrin, Jr., Y. Tian, R. Fu, C. V. Grant, E. Y. Chekmenev, W. E. Wieczorek, A. E. Dao, R. M. Hayden, C. M. Burzynski, R. M. Venable, M. Sharma, S. J. Opella, R. W. Pastor, M. L. Cotten, *J. Am. Chem. Soc.* **2014**, *136*, 3491–3504; d) M. Mihailescu, M. Sorci, J. Seckute, V. I. Silin, J. Hammer, B. S. Perrin, Jr., J. I. Hernandez, N. Smajic, A. Shrestha, K. A. Bogardus, A. I. Greenwood, R. Fu, J. Blazyk, R. W. Pastor, L. K. Nicholson, G. Belfort, M. L. Cotten, *J. Am. Chem. Soc.* **2019**, *141*, 9837–9853; e) U. Silphaduang, E. J. Noga, *Nature* **2001**, *414*, 268–269.

[8] H. I. Okur, J. Hladilkova, K. B. Rembert, Y. Cho, J. Heyda, J. Dzubiella, P. S. Cremer, P. Jungwirth, *J. Phys. Chem. B* **2017**, *121*, 1997–2014.

[9] a) A. Mishra, G. H. Lai, N. W. Schmidt, V. Z. Sun, A. R. Rodriguez, R. Tong, L. Tang, J. Cheng, T. J. Deming, D. T. Kamei, G. C. Wong, *Proc. Natl. Acad. Sci. USA* **2011**, *108*, 16883–16888; b) N. W. Schmidt, M. Lis, K. Zhao, G. H. Lai, A. N. Alexandrova, G. N. Tew, G. C. Wong, *J. Am. Chem. Soc.* **2012**, *134*, 19207–19216.

[10] B. S. Perrin, Jr., A. J. Sodt, M. L. Cotten, R. W. Pastor, *J. Membr. Biol.* **2015**, *248*, 455–467.

[11] G. C. L. Wong, *Curr. Opin. Colloid Interface Sci.* **2006**, *11*, 310–315.

[12] L. P. Kozlowski, *Biol. Direct* **2016**, *11*, 55.

[13] R. Gautier, D. Douguet, B. Antonny, G. Drin, *Bioinformatics* **2008**, *24*, 2101–2102.

[14] a) N. Y. Yount, D. C. Weaver, E. Y. Lee, M. W. Lee, H. Wang, L. C. Chan, G. C. L. Wong, M. R. Yeaman, *Proc. Natl. Acad. Sci. USA* **2019**, *116*, 6944–6953; b) E. Y. Lee, B. M. Fulan, G. C. Wong, A. L. Ferguson, *Proc. Natl. Acad. Sci. USA* **2016**, *113*, 13588–13593.

[15] B. Taheri, M. Mohammadi, I. Nabipour, N. Momenzadeh, M. Roozbehani, *PLoS One* **2018**, *13*, e0206578.

[16] Z. Wu, Q. Cui, A. Yethiraj, *J. Phys. Chem. B* **2013**, *117*, 12145–12156.

[17] a) A. Mishra, K. P. Tai, N. W. Schmidt, A. J. Ouellette, G. C. Wong, *Methods Enzymol.* **2011**, *492*, 127–149; b) N. W. Schmidt, A. Mishra, G. H. Lai, M. Davis, L. K. Sanders, D. Tran, A. Garcia, K. P. Tai, P. B. McCray, A. J. Ouellette, M. E. Selsted, G. C. Wong, *J. Am. Chem. Soc.* **2011**, *133*, 6720–6727; c) N. W. Schmidt, G. C. Wong, *Curr. Opin. Solid State Mater. Sci.* **2013**, *17*, 151–163.

[18] A. Som, L. Yang, G. C. Wong, G. N. Tew, *J. Am. Chem. Soc.* **2009**, *131*, 15102–15103.

[19] M. W. Lee, S. Chakraborty, N. W. Schmidt, R. Murgai, S. H. Gellman, G. C. Wong, *Biochim. Biophys. Acta Biomembr.* **2014**, *1838*, 2269–2279.

[20] R. N. Lewis, R. N. McElhaney, P. E. Harper, D. C. Turner, S. M. Gruner, *Biophys. J.* **1994**, *66*, 1088–1103.

[21] P. E. Harper, S. M. Gruner, *Eur. Phys. J. E* **2000**, *2*, 217–228.

[22] a) D. Choi, J. H. Moon, H. Kim, B. J. Sung, M. W. Kim, G. Y. Tae, S. K. Satija, B. Akgun, C. J. Yu, H. W. Lee, D. R. Lee, J. M. Henderson, J. W. Kwong, K. L. Lam, K. Y. C. Lee, K. Shin, *Soft Matter* **2012**, *8*, 8294–8297; b) H. D. Herce, A. E. Garcia, J. Litt, R. S. Kane, P. Martin, N. Enrique, A. Rebolledo, V. Milesi, *Biophys. J.* **2009**, *97*, 1917–1925; c) S. Li, Y. Su, W. Luo, M. Hong, *J. Phys. Chem. B* **2010**, *114*, 4063–4069; d) S. Sharmin, M. Z. Islam, M. A. Karal, S. U. Alam Shibly, H. Dohra, M. Yamazaki, *Biochemistry* **2016**, *55*, 4154–4165; e) S. A. Akimov, P. E. Volynsky, T. R. Galimzyanov, P. I. Kuzmin, K. V. Pavlov, O. V. Batishchev, *Sci. Rep.* **2017**, *7*, 12152; f) M. Z. Islam, S. Sharmin, V. Levadnyy, S. U. Alam Shibly, M. Yamazaki, *Langmuir* **2017**, *33*, 2433–2443; g) E. Trofimenko, G. Grasso, M. Heulot, N. Chevalier, M. A. Deriu, G. Dubuis, Y. Arribat, M. Serulla, S. Michel, G. Vantomme, F. Ory, L. C. Dam, J. Puyal, F. Amati, A. Luthi, A. Danani, C. Widmann, *eLife* **2021**, *10*, e69832; h) M. Serulla, G. Ichim, F. Stojceski, G. Grasso, S. Afonin, M. Heulot, T. Schober, R. Roth, C. Godefroy, P. E. Milhiet, K. Das, A. J. Garcia-Saez, A. Danani, C. Widmann, *Proc. Natl. Acad. Sci. USA* **2020**, *117*, 31871–31881.

[23] a) S. Afonin, A. Frey, S. Bayerl, D. Fischer, P. Wadhwani, S. Weinkauf, A. S. Ulrich, *ChemPhysChem* **2006**, *7*, 2134–2142; b) T. Murayama, T. Masuda, S. Afonin, K. Kawano, T. Takatani-Nakase, H. Ida, Y. Takahashi, T. Fukuma, A. S. Ulrich, S. Futaki, *Angew. Chem. Int. Ed.* **2017**, *56*, 7644–7647; *Angew. Chem.* **2017**, *129*, 7752–7755.

Manuscript received: June 25, 2021
Accepted manuscript online: March 29, 2022
Version of record online: ■■, ■■

Research Articles

Peptides

W. Xian, M. R. Hennefarth, M. W. Lee, T. Do, E. Y. Lee, A. N. Alexandrova,* G. C. L. Wong* **e202108501**

Histidine-Mediated Ion Specific Effects Enable Salt Tolerance of a Pore-Forming Marine Antimicrobial Peptide

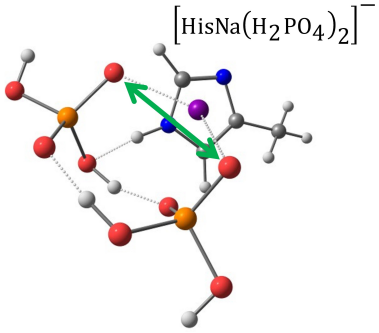

A combination of density functional theory, synchrotron small-angle X-ray scattering, mutational studies, and antimicrobial assays show that the histidine residues of a marine antimicrobial peptide coordinate sodium ions and the phosphate in headgroups of lipids to maintain the activity of the peptide at high salt concentrations. The placement of histidines in the α-helical conformation of the peptide is critical.